UHASSELT

KNOWLEDGE IN ACTION

Faculteit Wetenschappen

master in materiomics

Masterthesis

Optimizing elastin-like proteins and hyaluronic acid for hydrogel formation in tissue engineering applications

Lisa Cuypers

Scriptie ingediend tot het behalen van de graad van master in materiomics

PROMOTOR :

Prof. dr. Geert-Jan GRAULUS

Prof. dr. Virginie BITO

2023
2024

UHASSELT

KNOWLEDGE IN ACTION

www.uhasselt.be
Universiteit Hasselt
Campus Hasselt:
Martelarenlaan 42 | 3500 Hasselt
Campus Diepenbeek:
Agoralaan Gebouw D | 3590 Diepenbeek

UHASSELT

KNOWLEDGE IN ACTION

Faculteit Wetenschappen

master in materiomics

Masterthesis

Optimizing elastin-like proteins and hyaluronic acid for hydrogel formation in tissue engineering applications

Lisa Cuypers

Scriptie ingediend tot het behalen van de graad van master in materiomics

PROMOTOR :

Prof. dr. Geert-Jan GRAULUS

Prof. dr. Virginie BITO

Optimizing elastin-like proteins and hyaluronic acid for hydrogel formation in tissue engineering applications

Lisa Cuypers[1,], Niels Geysmans[1], Virginie Bito[2] and Geert-Jan Graulus[1]*

[1] Biomolecule design group, Institute for Materials Research, Hasselt University, Agoralaan-building D, 3590 Diepenbeek, Belgium
[2] Cardio & Organ Systems, Biomedical Research Institute, Hasselt University, Agoralaan, 3590 Diepenbeek, Belgium
E-mail: lisa.cuypers@student.uhasselt.be

Keywords: tissue engineering, injectable hydrogels, hyaluronic acid, elastin-like proteins, RGD, heparin-binding domains

Abstract: Every year, cardiovascular diseases are responsible for one-third of all global deaths. Following a myocardial infarction, the body is unable to regenerate damaged heart tissue, which can evolve into life-threatening heart failure. A promising way to restore lost heart function is through stem cell therapy. Unfortunately, these therapies show limited retention of the stem cells in the heart. This research project aims to synthesize injectable hydrogels with enhanced cell adhesion, which support stem cell proliferation and additionally integrate into the surrounding tissue to increase stem cell retention. To achieve this, hydrogels that mimic the extracellular matrix, consisting of the natural polymer hyaluronic acid (HA) and bio-inspired elastin-like protein (ELP), will be designed. RGD (arginine-glycine-aspartic acid) and heparin-binding cell adhesive domains are incorporated into the ELPs, and thermoresponsive properties are confirmed. However, only a 3.93 mg L^{-1} yield of the ELPs is achieved after purification. Therefore, hydrogels are made using a model system with oxidized HA and adipic acid dihydrazide. Observed dynamic and self-healing properties, and preliminary compression tests (Young's modulus of 10.80 ± 1.87 kPA) show promising results. By optimizing these materials, the first steps toward more efficient stem cell therapies for regeneration of damaged heart tissue are being taken.

Abstract in Dutch: Elk jaar zijn hart- en vaatziekten verantwoordelijk voor een derde van alle sterfgevallen wereldwijd. Na een hartinfarct is het lichaam niet in staat om het beschadigd hartweefsel te regenereren, wat kan leiden tot levensbedreigend hartfalen. Stamceltherapie is een veelbelovende manier om de verloren hartfunctie te herstellen. Helaas vertonen deze therapieën een beperkte retentie van de stamcellen in het hart. Dit onderzoeksproject is gericht op de synthese van injecteerbare hydrogels met verbeterde celadhesie, die de proliferatie van stamcellen ondersteunen en zich bovendien integreren in het omringende weefsel om de retentie van stamcellen te verhogen. Om dit te bereiken zullen hydrogels worden ontworpen die de extracellulaire matrix nabootsen, bestaande uit het natuurlijke polymeer hyaluronzuur (HA)

en het bio-geïnspireerde elastine-achtig eiwit (ELP). RGD (arginine-glycine-asparaginezuur) en heparine-bindende celhechtingsdomeinen worden in de ELP's ingebouwd en thermoresponsieve eigenschappen worden bevestigd. Na purificatie wordt echter slechts een opbrengst van 3.93 mg L^{-1} van de ELP's bereikt. Daarom worden reeds hydrogels gemaakt met behulp van een modelsysteem met geoxideerd HA en adipinezuurdihydrazide. Waargenomen dynamische en zelfhelende eigenschappen, en eerste compressietesten (Young's modulus van 10,80 ± 1,87 kPA) zien er veelbelovend uit. Door deze materialen te optimaliseren worden de eerste stappen gezet naar efficiëntere stamceltherapieën voor de regeneratie van beschadigd hartweefsel.

1 Introduction

Globally, cardiovascular diseases (CVDs) are the leading cause of death. In 2019, 32 % of all global deaths were caused by CVDs, most commonly by heart attacks and strokes. Additionally, in 2019, 38 % of the population under 70 died from CVDs.[1] The universal definition for a heart attack, or myocardial infarction (MI), states that: "MIs are caused by a decreased or complete cessation of blood flow to a portion of the myocardium."[2] This can cause heart failure as the heart becomes incapable of pumping blood around the body properly, which ultimately results in death. Common treatments for heart failure include lifestyle changes, like exercising, stopping smoking and drinking, and eating a healthy diet. These are most often combined with medicines such as blood thinners, beta-blockers, vasodilators, and possibly surgeries, e.g., stent procedures, angioplasty, bypass surgery, or, in the worst case scenario, a heart transplant. However, besides transplantation, all of these treatment methods are only aimed at slowing down the progression of the condition and controlling the symptoms instead of treating the direct cause of the heart failure.[3,4] Following injury, the damaged myocardium cannot regenerate as cardiomyocytes are terminally differentiated cells and therefore cannot proliferate.[5] Thus, in order to recover the functionality of the damaged tissue after an MI, replacement of these cardiomyocytes is essential.

One way to replace these damaged cardiomyocytes is through stem cell therapy.[6] Stem cells have the potential to differentiate into many different types of specialized, functionally mature cells inside the body. At the moment, numerous human clinical trials for treating heart failure using stem cell-based therapy have demonstrated promising results. However, to the best of my knowledge all of the stem cell treatments for heart failure are still investigational and have yet to become approved as these trials still contain some discrepancies and limitations.[7–9] One such limitation is stem cell retention after stem cell implantation. This retention is important as the donor cells should remain in the recipient's heart long enough to send paracrine signals to surrounding heart cells and proliferate themselves.[9,10] At the moment, this retention lies below 20 %.[10]

Cardiac atrial appendage stem cells (CASCs) are a promising candidate for myocardial repair because they show cardiomyogenic differentiation as well as stimulate blood vessel formation

by paracrine mechanisms.[11] Tissue engineering can be used to introduce these CASCs inside the body at the damaged site. The three key parameters of tissue engineering are (stem) cells that grow into new tissue, scaffolds to provide proper support for these cells, and growth factors to promote and facilitate the process of cell growth.[12] Thus, living cells can be incorporated in polymeric scaffolds, analogous to the natural extracellular matrix (ECM) in tissues, which share abundant similarities with hydrogels.

Hydrogels are insoluble networks of crosslinked polymers that can retain large amounts of water.[13] In particular, injectable hydrogels have proven attractive to deliver scaffolds and cells in a minimally invasive way to the desired place inside the patient's body. As a result, the uncomfortable pain and complications of traditional surgeries in already weak patients can be circumvented.[14] These hydrogels should conform to several design parameters such as biocompatibility, gelling mechanism, and certain mechanical properties. Biocompatibility is necessary to avoid damaging the stem cells and surrounding tissue. The gelling mechanism is especially important for injectable hydrogels, which should gel inside the body.[15] One approach uses a phase transition from solution to gel around the lowest critical solution temperature (LCST). When the temperature increases above a characteristic transition temperature T_t, the polymer's solubility decreases, and a sol-gel transition occurs. When the LCST is designed to be around the body temperature, the hydrogels will gel once injected into the body.[16] The mechanical properties of the hydrogels should be comparable to those of native cardiac tissues (8-15 kPa Young's modulus; Cardiac MRE measurements with 140 Hz vibrations[17,18]). Heart tissue must also be capable of withstanding repetitive loading and unloading cycles that result from the heart's beating.[18] These mechanical properties are closely related to cell adhesion and gene expression. Adhesion as well as migration and differentiation are greatly affected by the interactions of the cells with the hydrogels. Therefore, the polymers used for these hydrogels should be highly biocompatible and exhibit binding domains for optimal adhesion of the scaffolds to the tissues inside the body, which is especially important for stem cell retention.[10,15] For tissue engineering, hydrogels from natural polymers as well as synthetic polymers are being used.

The first component of the hydrogels explored in this research is hyaluronic acid (HA). HA is a natural polymer. It can be found in native ECM and is part of a group called glycosaminoglycans, consisting of amino acids and uronic sugars as basic units. HA is non-toxic, non-immunogenic, non-inflammatory, and mucoadhesive. Moreover, it regulates cellular processes like cell adhesion, proliferation, and differentiation by binding targeted cell surface receptors.[19] HA is currently being used in numerous applications in the biomedical field, like wound healing, cancer treatment, ophthalmology, cosmetics, drug delivery, and tissue engineering.[14,20] Some HA-based hydrogels have already been synthesized for the treatment of myocardial infarction in animal studies. E.g., Yoon S. J. et al. synthesized hydrogels via a Michael-type addition reaction between acrylated HA and thiol functionalized poly(ethylene glycol),[21] Lyu Y. et al. prepared injectable HA-based hydrogels through a Shiff base reaction between hydrazide functionalized HA and oxidized HA, loaded with functionalized mesenchymal stem cell aggregates.[22] In these

examples, HA is modified and/or combined with other components to tune the mechanical characteristics of the hydrogels as unmodified HA possesses poor mechanical properties.[14,19] In this thesis, the HA will be oxidized through a reaction with sodium periodate, which introduces aldehyde functional groups. The introduction of these aldehydes is needed to form the hydrogel as will be described later.

The second component of the hydrogels are elastin-like proteins (ELPs). ELPs are synthetic polymers inspired by tropoelastin, consisting of pentapeptide repeat valine-proline-glycine-X-glycine $(VPGXG)_n$ with X any amino acid except proline. When introducing lysine as the X amino acid, site-specific and covalent crosslinking can occur with a primary amine. This will be used to functionalize the ELPs with hydrazine groups. ELPs are biocompatible, biodegradable and non-immunogenic. Due to their recombinant character, it is possible to modify the ELP sequences to introduce lysine residues, control the lengths of the constructs, and incorporate cell adhesive domains.[13] The well-known cell interactive RGD peptide (arginine-glycine-aspartic acid) will be inserted for cell adhesive properties.[23] In this project, the aim is to insert heparin-binding domains (HBD) alongside the RGD cell adhesive domains into the ELPs. HBD consists predominantly of arginine residues. These basic amino acids are protonated at physiological pH and are therefore expected to interact electrostatically with the negatively charged components of the ECM (e.g. polysaccharides heparan sulfate or HA).[24] It is expected that this will facilitate the integration of the hydrogel into the surrounding native tissue. Furthermore, HBD promotes focal adhesion formation.[25] As a result, it is expected that the combination of the two adhesive domains, RGD and HBD, will enhance cell adhesion, proliferation, and integration of the hydrogel. In each ELP, four cell binding domains will be inserted. These will be referred to as tetramers in this thesis. Moreover, ELPs are thermoresponsive and show LCST behavior and thus can reinforce the hydrogel by aggregation above the characteristic T_t.[13,23]

After both components are acquired, they will be combined for the formation of ELP-HA hybrid hydrogels. The first network of these hydrogels is formed via the dynamic covalent hydrazone linkages between the modified HA and ELPs.[6] These linkages are attained through click chemistry, namely a Shiff base reaction between the aldehyde groups on HA and the hydrazine groups on the ELPs. The dynamic character of these linkages provides self-healing and injectability properties of the hydrogels.[13,26] Furthermore, aggregation of the thermoresponsive ELPs will form a second network of the hydrogel once they are injected into the body. An overview of this concept is shown in **Figure 1**. For this thesis however, the focus will be on optimizing and characterizing the components of the hydrogel separately to make way for the synthesis of covalently adaptable ELP-HA hybrid hydrogels with secondary thermoresponsive crosslinking for injectable stem cell delivery in the future.

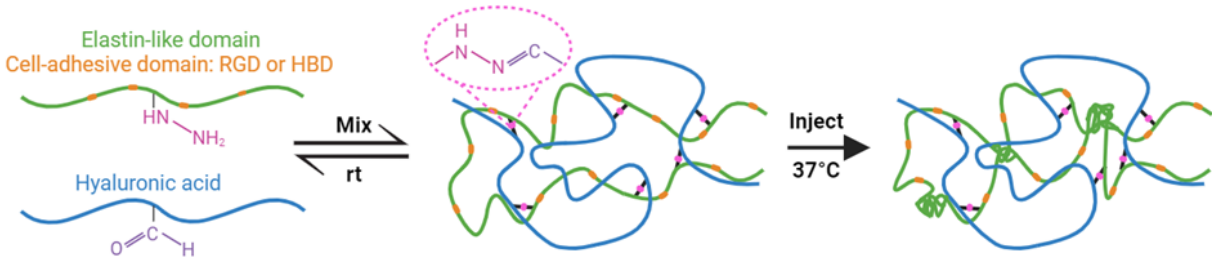

Figure 1. Hydrogel concept: After mixing the modified hyaluronic acid and elastin-like proteins (ELPs) a dynamically crosslinked network is formed via reversible hydrazone linkages, as shown in pink. Once the gel is injected into the body, a second network will be formed in the hydrogels by aggregation of the ELPs above 37 °C.

2 Results and discussion

2.1 Tetramer plasmid library expansion

The HHHR tetramer was one of the remaining tetramer inserts that still needed to be synthesized to complete the ELP library, see **Table S1**. A conceptual figure of the whole process can be found in the supporting information, **Figure S1**. This HHHR tetramer was synthesized via recursive directional ligation by plasmid reconstruction (PRe-RDL) in a pUC18 cloning vector, starting from dimer sequences HH and HR that were already designed in the research group. This process took place in two stages. First, restriction digestion with type II restriction endonucleases was used to purify the dimer DNA fragment from the parent vector, resulting in complementary ends of the target plasmid and insert. These oligomers were ligated together to reconstitute a functional tetramer plasmid in a cloning vector.[27] The tetramer insert was transformed into TOP10 competent cells and four colonies were picked and grown. A polymerase chain reaction (PCR) was performed and the PCR products were separated with electrophoresis on 1 % agarose gels, as can be seen in **Figure 2A**. The gel shows slight bands around 1200 base pairs (bp) for all samples. Therefore, all samples were sent for sequencing.

When the sequences of the inserts were confirmed, the ELP inserts were transferred from the pUC18 cloning vector into a pET15b expression vector through recursive directional ligation (RDL). In RDL, recursive addition of an oligomer with another compatible DNA sequence was done stepwise by ligation of an insert with a compatible linearized parent vector.[27] In this case, the linearized vector was the pET15b vector, and the insert consisted of the HHHR tetramer sequence. Once again, the tetramer insert was transformed in TOP10 competent cells and four colonies were picked and grown. A PCR reaction was performed and the PCR products were separated with electrophoresis on a 1 % agarose gel, which can be seen in **Figure 2B**. On this gel, the first loaded sample is an empty pET15b vector and the second loaded sample is the RHHR tetramer in pET15b vector. These were added as a control to check if the transfer in the pET15b vector was accomplished for the newly ligated tetramers. Only the fourth PCR sample of HHHR showed a band at 1200 bp for a ligated tetramer. Tetramer ligation for this sample was

verified by Sanger sequencing. For the other samples, a band at the same height of the empty pET15b vector is still visible, thus ligation did not succeed. The confirmed tetramer sequence in the expression vector could now be transformed in different strains of *Escherichia coli (E. coli)* competent cells e.g. BLR(DE3), BL21(DE3), BL21(DE3)PLysS, and Rosetta^{TM}(DE3).

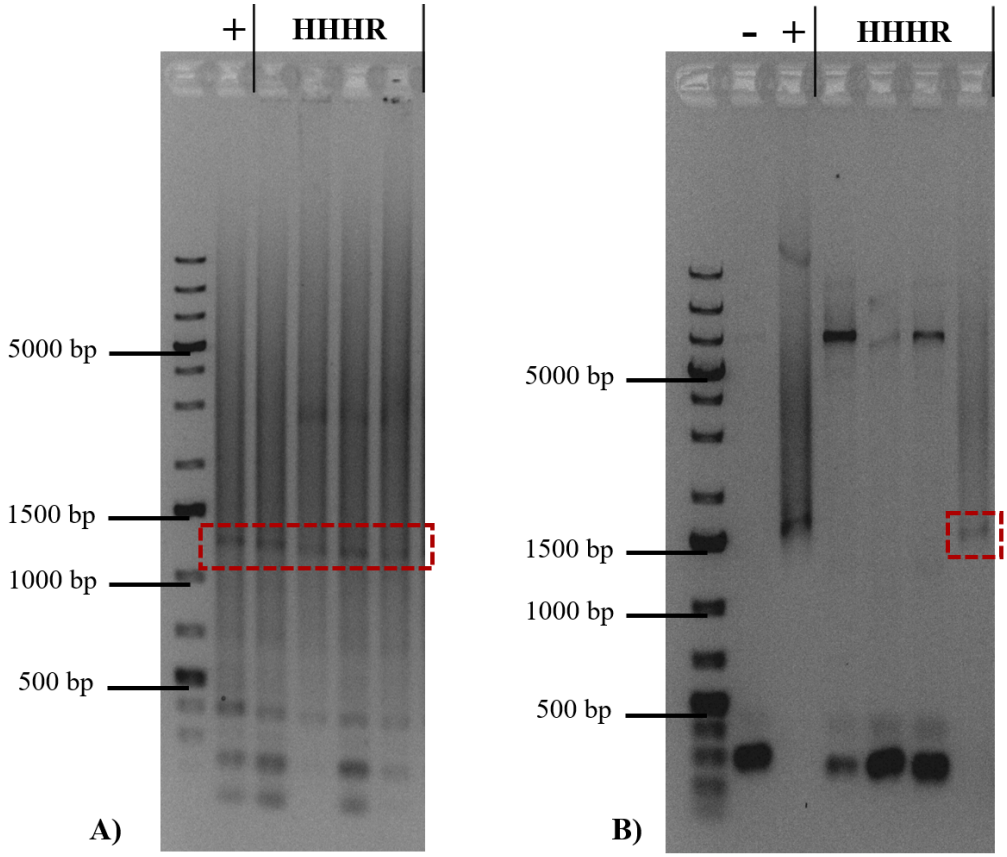

Figure 2. Confirmation of successful recursive directional ligation. **A)** Agarose gel showing the final length of the ELP HHHR plasmid, around 1200 bp, shown in the red box. The RHHR tetramer in the pUC18 vector is added as a positive control (+). **B)** Agarose gel showing the final length of the ELP HHHR plasmid incorporated in the pET15b expression vector. An empty pET15b vector and RHHR incorporated in this expression vector are added, respectively, as negative (-) and positive (+) control. The fourth HHHR tetramer matches the positive control, as indicated in the red box. For both gels, a 1 % agarose gel in TAE buffer was run at 100 V for 60 min, with the GeneRuler 1 kb plus ladder. The gels are stained with Midori Green Direct Stain.

2.2 ELP purification of RRRR and HHHH tetramer

In this project two tetramers, namely the RRRR and HHHH variant, were cultivated via bacterial growth and purified. The RRRR tetramer was used as a reference based on research results from the Heilshorn Biomaterials Group at Stanford University.[13,28] The HHHH tetramer was the onset for the use of HBD adhesive domains in ELPs. The RRRR and HHHH tetramers were expressed in *E. coli* BLR(DE3) competent cells. The cell cultures were pelleted and these cell pellets were resuspended in B-PER^{TM}. Sodium dodecyl sulfate polyacrylamide gel

electrophoresis (SDS-PAGE) was performed to check the purification efficacy of the tetramers during different stages of the purification process. The results can be seen in **Figure 3**. The first step of purification of the resuspended cell lysates was immobilized metal affinity chromatography (IMAC). IMAC uses the interaction of the histidine-tag in the ELPs with nickel beads for affinity purification. After washing steps, imidazole is used as a competitive ligand for the elution of the ELPs from the column.[29] The lane with the IMAC sample consists of a pooled sample from the four elution fractions of the IMAC. The remainder of the pooled sample was used for inverse transition cycling (ITC). ITC purification is based on the phase transition temperature of the ELPs. First, a hot spin at 40 °C took place where the ELPs aggregated and could be found in the hot spin pellet (HSP). The T_t of the RRRR tetramer was found to be 33.9 °C in literature.[13] Nonetheless, to make sure that the T_t of our ELPs lies below 40 °C, 2.5 M sodium chloride was added to the samples. The HSP was resuspended in Milli-Q and followed by a cold spin at 4 °C. The ELP agglomerates disassemble, and they could now be found in the cold spin supernatant (CSS).[30] Fractions of the hot spin supernatant (HSS) and cold spin pellet (CSP) were also loaded onto the gel to check if there was some loss of protein during these purification steps.

For both the RRRR and HHHH tetramer, the protein was observed after IMAC around 45 kDa. This corresponds with the theoretical molecular weight of a protein consisting of 1200 base pairs, which is 44 kDA. When comparing the intensity of the bands at 45 KDa, the band of the RRRR tetramer is more dense than the HHHH tetramer, which indicates a higher ELP concentration of the RRRR tetramer. Nevertheless, the samples are not 100 % pure yet, as can be seen by the presence of other bands on the gel. These bands could be assigned to some cell debris that is left in the sample, or, in a less preferable case, some degradation products of the proteins. This could be checked with, for example, a Western blot which uses label antibodies specific to the protein of interest that could indicate the presence of degradation products.[31] After ITC however, almost no proteins with a molecular weight of 45 kDa could be observed for the HHHH tetramer. The vast majority of ELPs were still present in the CSP. The RRRR tetramer showed some remaining protein in the CSP, nevertheless there is a lot of protein isolated in the CSS. Still, some impurities were visible in the CSS sample, though multiple ITC cycles can help to improve the purity. Other techniques, such as anion exchange chromatography or organic extraction followed by precipitation of the protein, can also be looked at for purification purposes.

On the CSS sample of the RRRR tetramer, UV-Vis transmission measurements were performed to determine the T_t of the ELP. The results are displayed in **Figure 4**. First, the sample was heated to 43 °C. The transmission dropped between 34 and 36 °C, which means that the T_t was reached and the ELP aggregated, conform the literature.[13] When cooling the sample back to 25 °C, a similar curve of transmission in function of time could be found, which means that the ELP aggregates disassembled when the temperature dropped back below the T_t.

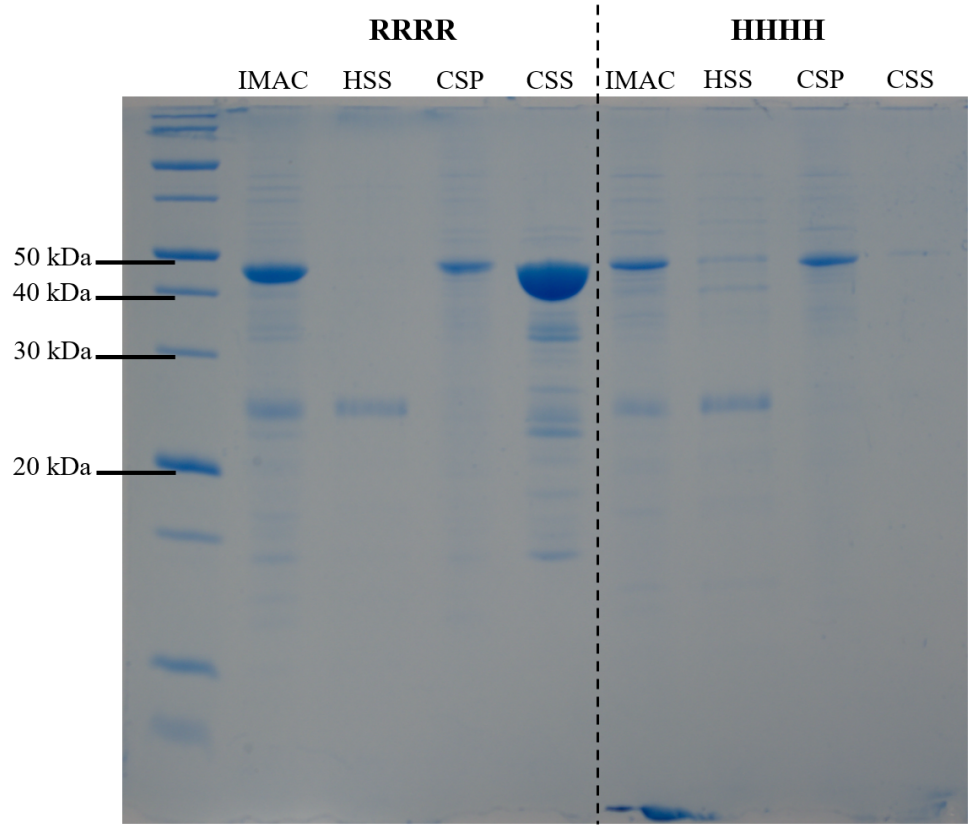

Figure 3. ELPs are purified through IMAC and ITC. SDS-PAGE gel loaded with samples of IMAC, hot spin supernatant (HSS), cold spin pellet (CSP), and cold spin supernatant (CSS). The SDS-PAGE gel was run at 180 V for 90 min, with the PageRuler^{TM} Unstained Broad Range protein ladder. The gel is stained with InstantBlue^{TM}. The ELPs have a molecular weight of 45 kDa. A band at 45 kDa is visible for the RRRR IMAC, CSP, and CSS samples, and for the IMAC and CSP samples of the HHHH tetramer.

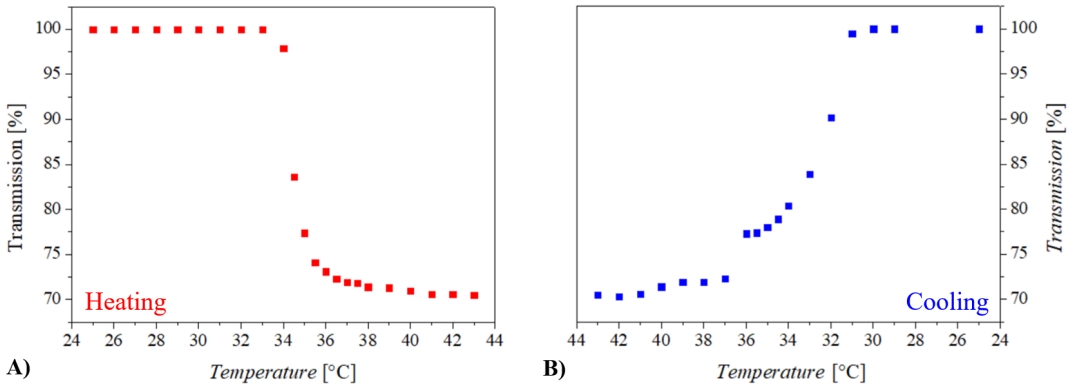

Figure 4. Verification of LCST behavior of the ELP. UV-Vis transmission measurements at 300 nm **A)** going from 25 °C to 43 °C (heating) and **B)** back from 43 °C to 25 °C (cooling) in steps of 1 or 0.5 °C. The transition temperature is situated between 34 and 36 °C. The heating and cooling show a similar curve in function of the temperature, which confirms the assembly and disassembly process of the ELPs into aggregates, respectively, above and below the transition temperature.

A bicinchoninic acid (BCA) assay was performed to measure protein concentration. Peptide bonds and some amino acids can reduce a cupric ion (Cu^{2+}) to a cuprous ion (Cu^{+}) via the biuret reaction under alkaline conditions. This property is used in the BCA assay method, as the sodium salt of BCA reacts with the cuprous ion generated by the peptide bonds to form a BCA-cuprous complex. This complex forms a deep blue color that can be measured with UV-Vis spectroscopy at 562 nm. The concentration of the protein is in direct relation with the intensity of the color at 562 nm.[32,33] The concentration of the RRRR tetramer in the CSS was measured at 0.786 mg mL^{-1}. Overall, taking into account the sample size of the purified sample and the amount of culture medium used for the bacterial cultivation, the yield of the RRRR ELP was 3.93 mg L^{-1} medium. This is low compared to the 50 mg L^{-1} yield obtained in the Heilshorn Biomaterials Group.[28] This low concentration could be due to some irregular folding of the protein structure as a result of the use of unique codons in the DNA sequence. In hopes of upscaling the ELP production, a new construct will thus be explored. Similar steps and experiments to those described above will be conducted with this new construct to create a new plasmid library in order to hopefully improve the production of ELPs via bacterial growth. However, this is beyond the scope of this thesis project.

2.3 Oxidation of hyaluronic acid

Aldehyde groups were introduced to HA through an oxidation reaction with sodium periodate, which can be seen on the left-hand side of **Figure 5**. Through ^{1}H-NMR (right-hand side of **Figure 5**) the reaction product was confirmed. In both the NMR of the HA and the NMR of the oxidized HA (oHA), characteristic peaks of the sugar rings could be seen at 3.0 - 4.0 ppm, as well as the *N*-acetyl peak at 1.9 ppm. In the oHA spectrum, three signals appeared between 4.8 - 5.1 ppm, which correlate to hemiacetal protons formed due to the reaction of the aldehyde groups with water or nearby hydroxyl groups.[34–36] Confirmation of the oxidation reaction could be done via the small signal at 9.5 ppm, which corresponds to an aldehyde functional group. Another method to validate the oxidation reaction is through fourier transform infrared spectroscopy (FTIR). FTIR spectra of unmodified HA, as well as the 1:1 (HA:$NaIO_4$) and the 1:2 oHA batch can be seen in **Figure 6**. Characteristic peaks of the HA could be observed, i.e. O-H stretch vibration of OH groups and stretching of the NH in the *N*-acetyl group at 3400 cm^{-1}, symmetric and asymmetric stretching of the CH_3 and CH_2 groups at 2900 cm^{-1}, stretching of the COOH and shoulder of the NH (*N*-acetyl group) at 1600 cm^{-1}, symmetric and asymmetric bending of CH_3 at respectively 1380 and 1420 cm^{-1} and the scissoring bending of CH_2, and all C-O stretching at 1000 cm^{-1}. However, the most important peak in this FTIR spectrum of oHA was the shoulder at 1730 cm^{-1}, which correlates to the C = O symmetric vibration of the aldehyde moieties according to literature (zoomed part of Figure 6).[13,34]

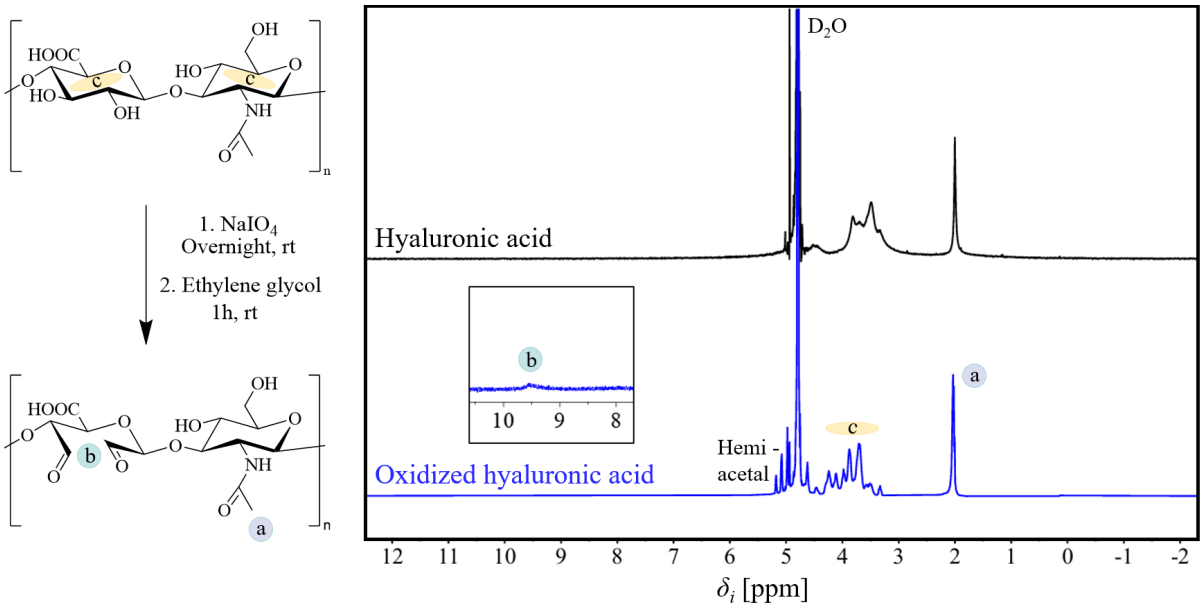

Figure 5. Oxidation of hyaluronic acid. Left-hand side: Scheme of the oxidation reaction of HA. First sodium periodate is added to oxidize the HA and introduce aldehyde functional groups. Whereafter, ethylene glycol is added to stop any unreacted periodate from oxidizing the HA further. Right-hand side: ^{1}H-NMR in D_2O (400 MHz, 298 K). The NMR spectra are normalized at the 2.0 ppm peak. The zoomed part shows a signal at 9.5 ppm, which confirms the presence of the aldehyde functional group.

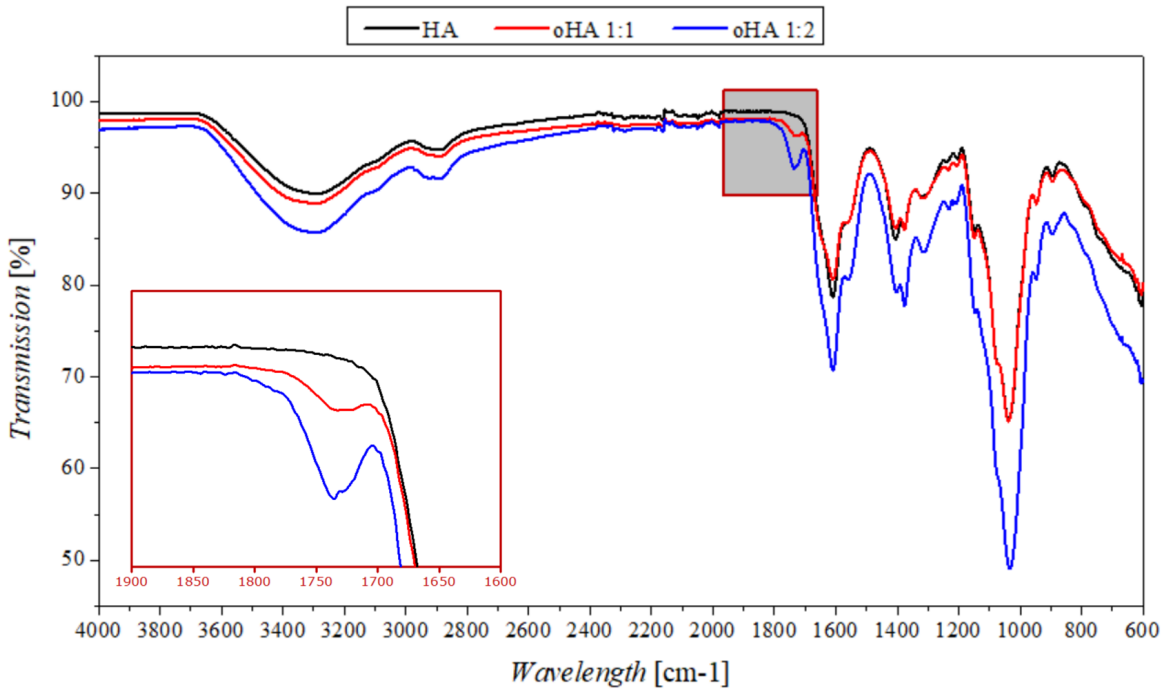

Figure 6. FTIR spectra of hyaluronic acid compared to the 1:1 and 1:2 HA:oxidant batches of oxidized HA. The shoulder at 1730 cm^{-1} confirms the presence of aldehyde groups and thus validates the oxidation reaction.

2.4 Degree of oxidation (DO) of hyaluronic acid

2.4.1 2,4,6-trinitrobenzene sulfonic acid (TNBS) assay

TNBS assays can be used to quantify the degree of HA oxidation. oHA reacts with an equimolar amount of *tert*-butyl carbazate (*t*BC) in 1 % aqueous trichloroacetic acid solution. Aqueous TNBS solution will then be added to react with the excess *t*BC. UV-Vis absorption measurements are used to calculate the amount of unreacted *t*BC using a standard calibration curve. This result can then be converted into dialdehyde content to obtain the degree of oxidation (DO) of HA.[13,37–39] However neither by following the Thermofisher protocol,[37] nor by procedures based on reported protocols in papers,[13,38] a linear calibration curve could be obtained for aqueous *t*BC solutions. It was possible to obtain a linear calibration curve for a model system with glycine (**Figure S2**).[38] Nevertheless, this could not be translated into the application at hand.

2.4.2 3-methyl-2-benzothiazolinone hydrazone (MBTH) assay

The 3-methyl-2-benzothiazolinone hydrazone (MBTH) assay is a colorimetric method for measuring, among other things, low-level residual aldehyde polysaccharide-protein conjugates. This colorimetric detection happens in two stages. First, MBTH is left to react with the aldehydes, to form azine. Next, ferric ammonium sulfate forms a reactive cation with the excess MBTH, which can lead to a reaction between this cation and the formed azine. This final reaction leads to the formation of the blue chromophore formazan, which absorbs light at 610 nm.[40] A calibration curve was obtained with *para*-formaldehyde and used to calculate the DO of oHA (**Figure S3**). The DO of oHA batches with varying amounts of sodium periodate added to the reaction mixture were measured. The DO of the 3:1 HA:$NaIO_4$ batch was calculated at 2.24 %, the 2:1 batch at 3.23 %, the 1:1 batch at 3.04 %, and the 1:2 batch at 1.09 %. However, it was expected to get an increase in DO with increasing $NaIO_4$ reagent, and the formazan complex also seemed to have a more intense blue color as more sodium periodate was left to react with the HA, as can be seen in **Figure S4A**. This discrepancy between theoretical expectations and these results could be explained by the observed blue precipitation in centrifuged samples (**Figure S4B**). This precipitation was not observed in the samples for the calibration curve. The occurrence of precipitation seemed to increase with increasing $NaIO_4$ content. Therefore, measurements of the 1:1 and 1:2 batches were repeated after mixing the precipitation again, and a DO of, respectively, 4.48 % and 2.04 % were obtained. However, the precipitate did not resolve completely after mixing again, which also could have led to these inconsistent results. Different dilutions of oHA with a theoretical aldehyde concentration of 6 mM (assuming 100 % DO), starting from 1/2 to 1/200, were also tried in case of saturation by formazan in the samples, yet the precipitation was still present. These results are, therefore, still not conclusive in the determination of the DO. When 50 mM of ethylenediaminetetraacetic acid was added to the precipitation and shaken overnight, the precipitate dissolved completely, and the solution

turned into an orange color (**Figure S4C**). After centrifugation of this sample, their was no new precipitation visible. This could mean that the observed blue precipitation is due to the complexation of Fe^{3+} with the oHA directly. A next step in optimizing this assay could thus be adjusting the amount of Fe^{3+} used.

2.4.3 Sodium cyanoboroydride ($NaCNBH_3$) reduction

Another way to determine the aldehyde content relies on ^{1}H-NMR spectroscopy. For this method, oHA reacted with an excess of *t*BC, followed by a reduction with $NaCNBH_3$. The degree of oxidation could then be obtained by comparing the NMR signal of the *tert*-butyl group of *t*BC at 1.4 ppm and the *N*-acetyl group of HA at 2.0 ppm.[41] For the 1:1 HA:oxidant a DO of 7.83 % (**Figure S5**) was calculated and 22.78 % oxidation for the 1:2 batch (**Figure S6**) was obtained. These DOs increase with an increasing amount of oxidant added in the reaction, as would be expected, contrary to the MBTH assay results. The DOs obtained with the MBTH assay are also much lower, with 3.04 % for the 1:1 instead of 7.83 %, and 1.09 % compared to 22.78 % for the 1:2 batch. However, cyanoborohydride is a very toxic chemical, and the reaction itself can cause an explosion due to the development of H_2 gas. Hence, optimizing other DO-determining methods remains valuable. Moreover, these alternatives could validate the results obtained via the $NaCNBH_3$ reduction.

2.5 Different approach for hyaluronic acid modification with aldehyde functional group

Another way to introduce an aldehyde functional group onto the HA, instead of through an oxidation reaction that results in ring-opening of the HA backbone, is via modification of the carboxylic acid group.[28] Before this reaction could be set up, 4-azidobenzaldehyde needed to be synthesized from 4-nitrobenzaldehyde. This was done through a reaction with sodium azide (**Scheme S1**). When adding the sodium azide to the 4-nitrobenzaldehyde, the mixture went from a yellow color to red to deep purple. During washing steps, the product became yellow again, and after drying, purification via silica gel chromatography, and removing the solvent, an ocher yellow liquid was obtained. The product (yield 30.4 %) still contained some particles that were not dissolved, nonetheless on the ^{1}NMR (**Figure S7**) the product seemed pure.
Now the modification of the HA could be set up. The first step in this reaction scheme was an 1-(3-(dimethylamino)propyl)-3-ethylcarbodiimide hydrochloride (EDC) - *N*-hydroxysuccinimide (NHS) coupling of propargylamine on the HA's carboxyl functional group to form an alkyne end-functional group (**Scheme S2A**). Hereafter, a copper-click chemistry reaction happened between the alkyne and 4-azidobenzaldehyde (**Scheme S2B**). After the click reaction, the final product was dialyzed against deionized water and lyophilized. Unfortunately, the reaction could not be confirmed via ^{1}H-NMR as characteristic peaks of the benzene and aldehyde could not be observed (**Figure S8B**). An FTIR measurement showed the shoulder peak at 1730 cm^{-1} (**Figure S9**). However, this shoulder was already visible in FTIR spectrum of the alkyne functionalized

HA. This could suggest that the peak at 1730 cm^{-1} is not the C=O symmetric vibration of the aldehyde functional group. Further investigation of this signal will be needed as this could also impact the characterization method of the oHA synthesized via sodium peroxide. Moreover, the characteristic peak around 2100 cm^{-1} of an end-functional alkyne could not be observed. The NMR measurements of the alkyne modified HA were not sufficient to confirm the presence of the alkyne group (**Figure S8A**). It seems that the reaction did not occur properly, if there were any functionalization, it would probably be at a very low percentage. Further characterization will be needed to assess this compound and the synthesis protocol will need to be optimized.

2.6 Composition and characterization of HA-hydrogels

2.6.1 Hydrogel composition

As the ELPs still need to be upscaled, hydrogels of the oxidized HA with adipic acid dihydrazide (ADH) were made for proof of principle. For both components, stock solutions in phosphate buffered saline were made with percentages ranging from 1 w/v % to 6 w/v % oHA and 1 w/v % to 8 w/v % ADH. Gels were made by mixing these stock solutions in a 4:1 volume ratio.[42] It was observed that a 2:1 molar ratio of aldehyde groups to hydrazide functional groups and batches with higher theoretical DO, gave the best result of gels with proper gelation.

2.6.2 Dynamic character and self-healing properties

To test the dynamic character and self-healing properties of the hydrogels, two oHA-ADH hydrogels with the same composition, 1:1 oHA 6 w/v % with ADH 4 w/v %, were cast. The gels were stained with two different food colorings. Blue and red were chosen for a good contrast. After complete gelation, the two hydrogels were cut in two with a scalpel and halves with different colors were placed next to each other. After one hour, a purple band became visible which means that hydrazone linkages were formed between the red and blue hydrogel halves. This experiment is presented in **Figure 7A**. **Figure 7B** shows that when picking the gel up with the blue side, the gel could be picked up as a whole which confirms the forming of new hydrazone linkages and self-healing properties of the hydrogels.

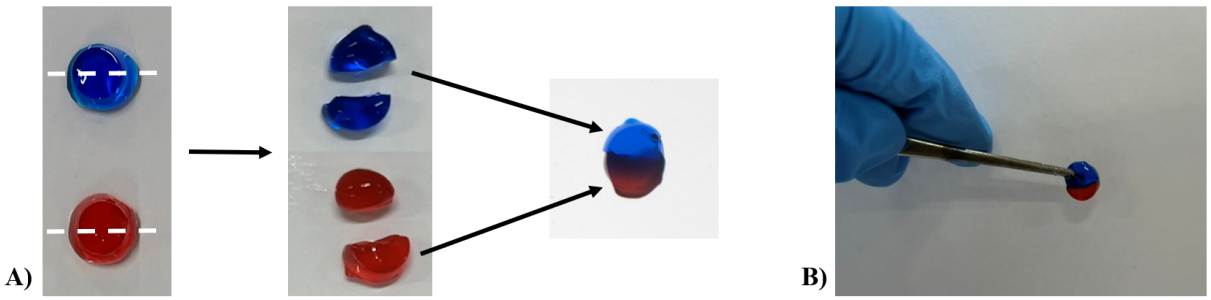

Figure 7. Testing of dynamic and self-healing properties of the hydrogel. The hydrogels consist of 6 w/v % oHA and 4 w/v % ADH in a 4:1 volume ratio, with red and blue food coloring. **A)** The hydrogels were cut in half with a scalpel, and then halves with opposite colors were placed next to each other. A purple band becomes visible, confirming the hydrogels' dynamic and self-healing properties. **B)** The two halves have formed new dynamic linkages and when picking them up with a tweezer, the gel can be picked up as a whole.

2.6.3 Compression testing

Preliminary unconfined compression tests were performed in triplicate on hydrogels with the 1:1 oHA 6 w/v % and ADH 4 w/v % composition, results can be seen in **Figure S10**. The Young's modulus was calculated to be 10.80 $\pm$ 1.87 kPA. The gels broke at 80.58 $\pm$ 6.85 % and the stress at break was 1517.20 $\pm$ 279.46 kPA. This large standard deviation could be due to some small bubbles that were present in the gels. For further compression and tensile testing, optimization of the hydrogel formation is required to obtain homogenous hydrogels that gel easily in the appropriate molds.

In order to compare the results of different batches of oHA, it is essential to determine the actual molecular weight of the different oHA batches. Oxidation via sodium periodate cleaves a sugar ring in the backbone of the HA, resulting in a lowering of the molecular weight. This molecular weight will influence the w/v % needed for the hydrogels, and the mechanical properties. Additional testing of the mechanical properties via rheology and injectability measurements will also be needed for further characterization of the hydrogels. Furthermore, swelling and degradation tests of the hydrogels should also be conducted.[41]

3 Conclusion

In this thesis, the ELP library was expanded, and ELP expression and purification were performed. Furthermore, HA was oxidized and characterized. Proof of principle hydrogels were made, and preliminary tests were performed.
Expansion of the ELP plasmid library with the HHHR tetramer from dimers was successful in a pUC18 and pET15b vector via recursive directional ligation. These results were confirmed via Sanger sequencing. Furthermore, different purification and characterization methods were performed on the ELP expression of the RRRR and HHHH tetramers. The HHHH tetramer showed

a loss of the ELPs during the ITC purification steps and an overall lower protein concentration than the RRRR tetramer on SDS-PAGE. For the RRRR tetramer a concentration of 0.786 mg mL^{-1} was obtained after IMAC and ITC purification via BCA assay, which corresponds to an ELP yield of 3.93 mg L^{-1} medium. After these purification steps, there were still some impurities left, and further purification will thus be needed. Nevertheless, the RRRR sample could be used to test the LCST behavior of the ELPs. ELP aggregation above T_t was confirmed using UV-Vis transmission measurements and the T_t was determined to be between 34 - 36 °C.
Next HA was modified through an oxidation reaction. ^{1}H-NMR and FTIR confirmed the presence of aldehyde functional groups on the oHA. In order to obtain the degree of oxidation, several methods were tried. TNBS assays were performed without any luck, even the calibration curve could not be obtained for the application at hand. Next MBTH assays were explored. Linear calibration curves were obtained, nonetheless this method still needs to be optimized for accurate determination of the degree of oxidation as blue precipitation is observed. A possible solution could be improving the amount of Fe^{3+} used in the assay, as it seems the precipitation corresponds to complexation of these ions with the oHA. The oxidation degree could be determined via ^{1}H-NMR after a reaction with *tert*-butyl carbazate followed by a reduction reaction with $NaCNBH_3$ and was determined to be 7.83 % for a 1:1 oHA batch, and 22.78 % for the 1:2 oHA, which is in line with expectations considering the amount of reacted oxidant. However, in order to validate these results, it would be best to optimize the MBTH assay. A second method to introduce an aldehyde functional group was also explored. This synthesis relied on EDC-NHS coupling to introduce an alkyne functional group at the carboxylic acid group of the HA, followed by copper click chemistry between the introduced alkyne and azidobenzaldehyde. However, further characterization of this product will be needed to compare both methods for the introduction of an aldehyde group to the HA.
The ELP yield was too low for modification with a hydrazide group. Therefore a model system of oHA with ADH was used for testing hydrogels. The dynamic and self-healing properties via the hydrazone linkages could be observed for 6 w/v % oHA with 4 w/v % ADH hydrogels. Preliminary compression tests show promising results but in order to correlate these results to the materials, it is important that the molecular weight of each oHA batch will be accurately determined. Moreover, swelling tests, degradation of the hydrogels, and further mechanical testing i.e. rheology and injectability, will need to be conducted in the future to fully characterize the material.
When considering the ultimate goal of this research, one might argue that the fundamental framework has been established. The upscaling of the ELP production is of utmost importance if enough material is to be obtained to modify it with hydrazines for hydrogel formation. This will be done in the further course of this research, starting with a new DNA construct. Similar steps and experiments as the ones described in this thesis will be undertaken with this new construct in order to create a new plasmid library and produce ELPs with higher yields. These ELPs will then be modified with hydrazine functional groups and characterized. For the HA,

the main focus will first be on optimizing the methods for the determination of the degree of oxidation. When methods for the characterization of both the modified HA and ELPs are optimized, hydrogels with these components can be made. Ultimately, after thorough testing of these ELP-HA hydrogels, stem cells could be introduced. Cell viability and, eventually, stem cell retention could then be assessed to conclude this research.

4 Experimental methods

4.1 Materials

4.1.1 Elastin-like proteins

Tryptone, sodium chloride, and tris-HCl (pH 6.8) were purchased from VWR chemicals. M13/ pUC Forward and Reverse primer and the T7-term primers were acquired via Integrated DNA Technologies. Acetic acid, and 2-mercaptoethanol were purchased from Acros Organics. The Midori Green Direct stain was acquired at Nippon Genetics. InstantBlue™ Coomassie Protein Stain was bought at Abcam, and Coomassie Brilliant Blue was purchased at Pierce. From Merck, (SIGMA, Sigma-Aldrich, Sigma Life Sciences) ethylenediaminetetraacetic acid (EDTA) disodium salt dihydrate, tris buffer (pH 8.45), *N,N,N',N'*-tetramethylethane-1,2-diamine, ammonium persulfate, sodium phosphate, 2-(*N*-morpholino)ethanesulfonic acid, were purchased. All other used products were purchased, and used without modification at ThermoFisher Scientific (Fisher BioReagents, Fisher Scientific, Thermo Scientific, Thermo Scientific Chemicals, ThermoFisher Scientific, Fisher Chemical)

4.1.2 Hyaluronic acid

Sodium periodate was acquired via Honeywell. Ethylene glycol was purchased at Merck (Aldrich). *N*-hydroxysuccinimide and 1-(3-(dimethylamino)propyl)-3-ethylcarbodiimide hydrochloride were purchased at Fluorochem. At Carbolution, propargylamine was purchased. β-cyclodextrin was acquired at BLD Pharmatech. *tert*-Butyl carbazate was purchased at TCI America. At Alfa Aesar, trichloroacetic acid was purchased. Potassium chloride was acquired at FLUKA. At VWR Chemicals, sodium chloride and potassium dihydrogen phosphate were purchased. 4-nitrobenzaldehyde, sodium azide, sodium ascorbate, sodium bicarbonate, sulfamic acid, *para*-formaldehyde, and sodium cyanoborohydride were acquired at Acros Organics. The ethylene glycol, copper sulfate, disodium phosphate, EDTA, picrylsulfonic acid, MES hydrate, and ferric ammonium sulfate dodecahydrate were purchased at Merck (Aldrich, Sigma-Aldrich, SIGMA, Sigma Life Science, and Sulpeco). All other used products were purchased, and used without modification at ThermoFisher Scientific (Fisher Chemicals, Fisher Scientific, Fisher Bioreagents, Thermo Scientific Chemicals)

4.2 Methods

4.3 Expanding the ELP plasmid library

4.3.1 General procedure

Glycerol stocks of the dimers in the pUC18 vector were inoculated on lysogeny broth (LB) agar plates (10 g L^{-1} tryptone, 5 g L^{-1} yeast extract, 10 g L^{-1} sodium chloride, and 15 g L^{-1} agar in Milli-Q water) containing 0.1 mg L^{-1} ampicillin (AMP). After colonies were picked and grown overnight in LB with AMP medium, the NucleoSpin® Plasmid EasyPure kit from Machery-Nagel was used to isolate the plasmid DNA. DNA restrictions were performed using FastDigest enzymes PspFI, XhoI and SalI, purchased from Thermo Fisher Scientific following the suppliers' instructions (**Table S2**).[43–45] Restrictions of the isolated plasmid DNA with these endonucleases were run (incubation at 37 °C overnight, inactivation at 80 °C for 10 minutes), and the products were put on an agarose gel to extract the DNA with the correct base pair lengths. This extraction of DNA from the gels was done using the NucleoSpin® Gel and PCR Clean-up kit from Machery-Nagel. Hereafter, T4 DNA ligase was used to reconstruct tetramer containing plasmids, as stated in the manufacturer protocol with a 3:1 molar ratio to vector (60 ng).[46] This ligation reaction was run in the thermocycler at 16 °C for 30 minutes, followed by 22 °C overnight, ending with 70 °C for 5 minutes. The ligated DNA samples were transformed into TOP10 *E. coli* competent cells, following the protocol as described by AddGene.[47] After growing these competent cells, the NucleoSpin® Plasmid EasyPure kit was used again to isolate the tetramer plasmid DNA. A PCR was run with M13/pUC Forward and Reverse primers flanking the constructed tetramer sequence using the Phire Hot Start II polymerase, in accordance with manufacturer's instructions (**Table S3**),[48]. Next, agarose gel electrophoresis was used to check the presence of the tetramer in the cloning vector before sending samples for sequencing. Once the sequences of the tetramer DNA plasmids were confirmed by Sanger sequencing (performed by LGC Genomics GmbH, 25 µL sample containing 100 ng/µL DNA), the transfer of the plasmids into expression vectors could start. This began with a restriction protocol on a pET15b vector as well as on the tetramer plasmid DNA. Linearization of the pET15B vector was performed based on the manufacturer's protocol (**Table S4**).[49] Restrictions of the tetramer plasmid with XhoI and SalI endonucleases were run (Table S2), and these samples were also put on an agarose gel to extract the DNA with the correct base pair lengths using the NucleoSpin® Gel and PCR Clean-up kit. Hereafter, T4 DNA ligase was used to reconstruct the ELP tetramer DNA sequences with the pET vector (3:1 molar ratio to vector, 50 ng), and the ligated DNA samples were transformed into TOP10 *E. coli* competent cells. Once again, a PCR, now with T7 and T7-term primers (Table S3), was performed with a following agarose gel electrophoresis to check the presence of the tetramers in the expression vector before sending samples for sequencing.

A Binder BD series incubator and IKA shaker KS 4000 i(c) control shaking incubator were used for bacterial cell growth. Restriction, ligation, and PCR reactions were performed in the Bio-Rad MJ Mini 48-Well Personal Thermal Cycler. The centrifuges used in the lab were the Eppendorf 5452 Minispin Centrifuge, the Eppendorf Centrifuge 5804 R, and the Eppendorf Centrifuge 5920 R, depending on the size of the Falcon™, and Eppendorf tubes®.

4.3.2 Agarose gel electrophoresis

1 % agarose was made with tris-acetate-EDTA (TAE) buffer. 1 L of TAE buffer contained 4.85 g tris base, 1.15 mL acetic acid, and 372.24 mg ethylenediaminetetraacetic acid (EDTA) disodium salt dihydrate. This TAE was also used as the running buffer. The used ladder was the GeneRuler 1 kb plus. 4 µL of nuclease-free water was added to 1 µL of the ladder to load onto the agarose gel. After restriction, the goal of these agarose gels was to extract DNA with the correct base pair length, thus the restriction samples were loaded onto the gel as a whole. After (colony) PCR, the agarose gels served merely as a checking tool therefore only 1 µL of sample after PCR was added to 4 µL of nuclease-free water. To stain the DNA, 10 % Midori Green Direct Stain was added to the samples prior to loading. The agarose gels were run at 100 V for 60 minutes with the Sub-Cell GT Cell from Bio-Rad.

4.4 Expression of ELPs

For the expression of the ELPs, a colony was picked from the agar plates and put in a growth medium overnight on a shaking incubator at 200 RPM and 37 °C. This starter culture could then be used to inoculate larger volumes of growth medium to increase the cell culture growth. When the optical density of the cell culture in the growth medium reached 0.6, the cells were induced with 1 mM isopropyl β-*d*-1-thiogalactopyranoside and allowed to express for at least three hours at 250 RPM and 37 °C or overnight at 30 °C on the shaking incubator. After expression, the culture was centrifuged to pellet the cells (2 minutes at 6800 G).
Hereafter, bacterial protein extraction reagent (B-PER™) could be used for the rupture of the bacterial cell wall in order to isolate the produced protein from the cell. When using B-PER™ to lyse the cells, 4 mL B-PER™ per g pellet was added, as well as 2 µL lysozyme and 2 µL DNAseI per mL B-PER™, and 1 protease inhibitor tablet per 10 mL B-PER™. The resuspended cell lysate was incubated at room temperature for 15 minutes. Next, this was centrifuged at 15 000 G for 5 minutes to pellet the largest part of the cell debris. The proteins could now be found in the supernatant.

LB growth medium, consisting of 10 g L^{-1} tryptone, 5 g L^{-1} yeast extract, and 10 g L^{-1} sodium chloride in Milli-Q water, was mainly used for the expression of the ELPs. For ELPs in the expression vector, terrific broth (TB) medium could be used. TB was made by dissolving 12 g tryptone, 24 g yeast extract, and 4 mL glycerol in 900 mL Milli-Q, and adding 100 mL of sterile

10x TB salts solution. The 10x TB salts solution consisted of 23.1 g L^{-1} KH_2PO_4 and 125.4 g L^{-1} K_2HPO_4 in Milli-Q. Both growth media contained 0.1 mg L^{-1} AMP.

4.5 Purification of ELPs

4.5.1 Immobilized metal affinity chromatography (IMAC)

HisPur™ Ni-NTA resin was added onto a gravity-flow column, and the column was equilibrated with two resin-bed volumes of equilibration buffer. The equilibration buffer contained 20 mM sodium phosphate, 300 mM sodium chloride, and 10 mM imidazole. Sample preparation consisted of mixing the protein extract with an equal volume of equilibration buffer. Thereafter, the sample was loaded onto the column and the flow-through was collected in a Falcon™ tube. Ten washing steps with two resin-bed volumes of wash buffer were performed, and the first and last washing steps were collected in different Falcon™ tubes to check the effectiveness of these steps with for example SDS-PAGE. The wash buffer contained 20 mM sodium phosphate, 300 mM sodium chloride, and 25 mM imidazole. Finally, the histidine-tagged proteins were collected by four elution steps using two resin-bed volumes of elution buffer. The elution buffer contained 20 mM sodium phosphate, 300 mM sodium chloride, and 250 mM imidazole. All these buffers had a pH of 7.4. Regeneration of the Ni-NTA is possible. Therefore, the column was washed with ten resin-bed volumes of MES buffer containing 20 mM 2-(*N*-morpholino)ethanesulfonic acid (MES) and 0.1 M sodium chloride. Followed by a washing with ten resin-bed volumes of Milli-Q. Lastly, ethanol and Milli-Q were added in a 50:20:30 ratio between Ni-NTA resin, ethanol, and Milli-Q to store the Ni-NTA as a slurry.[29]

4.5.2 Inverse transition cycling (ITC)

First of all, sodium chloride was added in a 2.5 M concentration to the sample (B-PER™ supernatant or elution fractions of IMAC). This was done to make sure that the T_t of the ELP was below 40 °C, which can be observed visually as the sample turbidity changes. This part of ITC is the hot spin at 40 °C with 15 000 G for 15 min. As the T_t was below 40 °C, the ELPs were aggregated and could be found in the hot spin pellet (HSP). The HSP was resuspended in Milli-Q (1 mL for 15 mL Falcon™ tube, 2 mL for 50 mL Falcon™ tube) and put on ice for at least 30 minutes. Hereafter, the Falcon™ tube was centrifuged at 4 °C with 15 000 G for 15 min, the so-called cold spin. The ELPs could now be found in the cold spin supernatant (CSS).[30] After each step, a 20 µL sample was taken of each fraction for comparison on SDS-PAGE.

4.6 Characterization and identification of ELPs

4.6.1 Sodium dodecyl sulfate polyacrylamide gel electrophoresis (SDS-PAGE)

SDS-PAGE is used for the confirmation of molecular weight and purity of the proteins. The resolving gel of the SDS-PAGE gel contained 12 % of acrylamide, and the stacking gel of the SDS-PAGE gel contained 4 % of acrylamide. Casting of these gels was done following standard protocol.[50] To 20 µL of the sample, 20 µL of 2x sample buffer was added, and the mixture was heated to 90 °C for 5 minutes in the thermocycler. Hereafter, the sample was centrifuged at 12 100 G for 1 minute. This sample buffer contained 100 mM tris–HCl (pH 6.8), 1 w/v % SDS, 4 v/v % 2-mercaptoethanol, 0.02 w/v % Coomassie Brilliant Blue and 24 w/v % glycerol. The ladder used for the SDS-PAGEs was the PageRuler™ Unstained Broad Range protein ladder. On the gel, 5 µL of the ladder and 10 µL of the samples were loaded. The gels were run in a tris-tricine running buffer at 180 V for 100 minutes with the Mini-PROTEAN ® Tetra Cell from Bio-Rad. The tris-tricine buffer contained 100 mM tris, 100 mM tricine, and 0.1 w/v % SDS, Afterward, the gels were soaked in InstantBlue® Coomassie Protein Stain to obtain blue staining of the gels. The thickness of the bands after staining, corresponds to the amount of protein present.[50]

4.6.2 Bicinchoninic acid (BCA) assay

In this project, the Pierce™ BCA Protein Assay Kit from ThermoFisher was used to perform the BCA assays. For reference, bovine serum albumin standards with concentrations between 2 µg mL^{-1} and 25 mg mL^{-1} were made. To 5 µL sample, 100 µL of working reagent (WR) was added. The WR was prepared by mixing 50 parts of BCA Reagent A with 1 part of BCA Reagent B and a clear and green WR was obtained. These samples were put on a shaking incubator at 100 RPM and 37 °C for 30 minutes. Afterward, the concentrations of the proteins were measured using the Nanodrop™ One Microvolume UV-Vis Spectrophotometer from ThermoFisher.[33]

4.6.3 UV-Vis measurements LCST behavior

UV-Vis transmission measurements can be used to determine the T_t of the ELPs. A decrease in transmission is observed at the T_t as the ELP aggregates and the solution becomes cloudy above this T_t. When cooling again, the transmission increases again to 100 %. The transmission of the ELPs was measured at 300 nm from 25 °C to 45 °C, and back down, in steps of 1 or 0.5 °C. At each temperature, the blank and the sample were measured. For these measurements, the Biochrom Ultrospec™ 9000 PC UV-Vis Spectrophotometer, with a deuterium UV lamp and a tungsten visible lamp as the light sources, was used in combination with the PolyScience 8010 Benchtop Digital Temperature Heating Circulator Controller accessory.

4.7 Oxidation of hyaluronic acid

Aldehyde groups were introduced to HA (1 840 000 g mol^{-1}) through a reaction with sodium periodate overnight. HA was dissolved in Milli-Q to obtain a 4 mg mL^{-1} concentration. An equimolar, to the number of active sites, quantity of sodium periodate (different HA:oxidant ratios were used for obtaining different oxidation levels) was added dropwise to the dissolved HA. This reaction was allowed to proceed by stirring in the dark at room temperature overnight. To inactivate any unreacted periodate, 500 µL ethylene glycol was added and the reaction was run at room temperature for 1 hour. Hereafter, the oxidized HA was dialyzed against deionized water for 3 days. Finally, the product was lyophilized and stored in a desiccator.[13] The product was characterized with 1H-NMR and FTIR spectroscopy.

The lyophilizer used was the Analis Alpha 1-2 LDplus from Martin Christ. ^{1}H-NMR were measured on the JEOL JNM-ECZS 400 MHz YH series instrument, where all spectra were referenced to the 0 ppm signal of tetramethylsilane. FTIR measurements were performed on the FT-IR Spectrometer Frontier of Perkin Elmer, with the PIKE MIRacle^{TM} Single Reflection ATR accessory containing a diamond with a ZnSe layer.

4.8 Modification of hyaluronic acid via copper click chemistry

4.8.1 Azido benzaldehyde synthesis

20 mmol 4-nitrobenzaldehyde and 40 mmol sodium azide were left to react overnight in 20 mL DMSO at 60 °C. The mixture was cooled down to room temperature. 200 mL diethyl ether was added, and the product was washed three times with water and a brine solution and dried over anhydrous Na_2SO_4. After evaporation of the solvent, the product was purified with a silica column chromatography using hexane and a hexane/ethyl acetate solvent mixture.[51]

4.8.2 Functionalization of HA

The first part consists of the functionalization of HA with alkyne via EDC-NHS coupling. 5 mg mL^{-1} HA was dissolved in MES buffer (0.2 M MES hydrate and 0.15 M sodium chloride; pH 4.5). An 0.8 equimolar quantity of propargylamine (pH 6.0), *N*-hydroxysuccinimide (NHS), and 1-(3-(dimethylamino)propyl)-3-ethylcarbodiimide hydrochloride (EDC) were added, and the reaction was left to stir overnight at room temperature. The HA-alkyne product was dialyzed against deionized water for three days and lyophilized. The HA-alkyne was dissolved in 10x PBS solution in a 5 mg mL^{-1} concentration, and 0.85 mg mL^{-1} β-cyclodextrin was added. After complete dissolution, 0.244 mM copper sulfate (diluted by 1/10 from 2.44 mM), and 4.52 mM sodium ascorbate (diluted by 1/10 from 45.2 mM) were added. 2 equivalents 4-azidobenzaldehyde per alkyne (100 mg mL^{-1} in DMSO) were then added dropwise. The re-

action was run under a N_2 atmosphere for 24 hours at room temperature in the dark. Hereafter, 50 mM EDTA solution was added in a 1:1 ratio and left to react for one hour at room temperature. Then, deionized water was added in a 1:5 ratio, and everything was filtered over a 0.2 µM syringe filter. The final product was dialyzed against deionized water for three days and lyophilized.[28]

4.9 Determining oxidation degree of hyaluronic acid

Agilent Technologies Cary 5000 UV-Vis-NIR Spectrophotometer with a deuterium arc UV lamp and a tungsten halogen visible lamp as light sources were used for the UV-Vis measurements performed in following assays.

4.9.1 2,4,6-trinitrobenzene sulfonic acid (TNBS) assay calibration curves

For the TNBS assay, 30 mM *tert*-butyl carbazate (*t*BC) reacts in a 1:1 ratio to oHA in 1 % aqueous trichloroacetic acid (TCA) for 24 hours at room temperature. For the calibration curves a 1:1 ratio of *t*BC to 1 % aqueous TCA was used. Concentrations between 3 and 30 mM of *t*BC in 1 % TCA were made. The TNBS solution consisted of 0.01 % picrylsulfonic acid solution in a 0.1 M $NaHCO_3$ buffer at pH 8.5. When following protocols from Thermofisher,[37] 250 µl of *t*BC, 250 µl TCA and 250 µl TNBS were left to react for two hours at 37 °C. Hereafter, 250 µl 10 % SDS and 125 µl 1 N HCl were added and the samples were measured with UV-Vis at 335 nm. For the protocol based on papers,[13,38] 25 µl *t*BC, 25 µl TCA and 500 µl TNBS were left to react for two hours at 37 °C. Thereafter, the sample was diluted with 1 N or 0.5 N HCl and measured at 335 and 340 nm.

4.9.2 3-methyl-2-benzothiazolinone hydrazone (MBTH) assay

The MBTH/SA solution was comprised of 5 mg mL^{-1} 3-methyl-2-benzothiazolinone hydrazone (MBTH) and 10 mg mL^{-1} sulfamic acid (SA) in deionized water. The FAS/SA solution consisted of 15 mg mL^{-1} ferric ammonium sulfate dodecahydrate (FAS) and 10 mg mL^{-1} SA in deionized water. Both solutions were stored at 5 °C and used within a week. For the standard calibration curve measurements of a serial dilution (1:2) starting from 0.3 mM to 0.00937 mM of *para*-formaldehyde were performed. The sample (*para*-formaldehyde or oHA), MBTH/SA, and FAS/SA solution were added in a 1:1:1 ratio. First, the sample was left to react with the MBTH/SA solution for one hour at room temperature. Hereafter, the FAS/SA solution was added, and the mixture was left to react for half an hour at room temperature. After this, the mixture was centrifuged at 2816 G for 5 minutes and measured with UV-Vis absorption measurements at 610 nm. As a blank control, deionized water was left to react simultaneously with the other samples.[40]

4.9.3 Sodium cyanoboroydride ($NaCNBH_3$) reduction

0.026 mM oHA and 0.26 mM tert-butyl carbazate were dissolved in a 0.1 M acetate buffer solution. After complete dissolution, 0.26 mM $NaCNBH_3$ in an equal amount of 0.1 M acetate buffer solution was added to the reaction mixture. The reaction was kept stirring for 24 h at room temperature. The product was then dialyzed against 0.1 M sodium chloride for 3 days and lyophilized. The oxidation degree was determined via the ratio of the *tert*-butyl group of the unreacted *tert*-butyl carbazate (1.4 ppm) and the *N*-acetyl group of the glucoaminoglycan of the HA (2.0 ppm) in the ^{1}H-NMR in D_2O.[41]

4.10 Hydrogel formation and compression tests

Phosphate buffered saline (PBS) contained 10 mM sodium phosphate, 2.68 mM potassium chloride, and 140 mM sodium chloride. oHA was dissolved in PBS in the range of 1 w/v % to 6 w/v %. ADH was dissolved in PBS in the range of 1 w/v % to 8 w/v %. Gels were made by mixing these stock solutions in a 4:1 volume ratio.[42]

Compression tests hydrogels were performed on the Shimadzu autograph AGS-X series universal tester of 500 kN. The top plate moved downward with a speed of 1 mm/min, pushing down on the hydrogels until break or 90 % strain, resulting in a stress-strain curve. The slope from the initial 20 % strain in the stress-strain curves gives the Young's modulus.[52]

Acknowledgments

First of all, I would like to thank my supervisor Drs. Niels Geysmans for his guidance and support during this thesis project. I also want to express my gratitude to my promotor prof. dr. Geert-Jan Graulus for giving me the opportunity to join the Biomolecule Design Group and his insightful advice during this project. This thesis internship was a great learning experience in an enjoyable working environment. Therefore, I am grateful to all the BDG members for their help, with a special thanks going out to Drs. Sander Driesen for his assistance in the lab. Additionally, I wish to thank Prof. Dr. Peter Adriaensens, Dr. Elien Derveaux, and Dr. Sander Smeets for their help with the NMR spectroscopy results. I would also like to acknowledge my co-promoter Prof. Dr. Virginie Bito. In addition, I would like to show my appreciation for Dr. Dorien Baeten, to whom we could always turn with our concerns and numerous questions regarding the master's program. Lastly, I am deeply thankful to my family and friends for their continuous support during this master's degree.

References

(1) World Health Organization Cardiovascular diseases (CVDs) https://www.who.int/news-room/fact-sheets/detail/cardiovascular-diseases-(cvds) (accessed Oct. 10, 2023).

(2) Thygesen, K. et al. *Circulation* **2007**, *116*, 2634–2653.

(3) National Health Service Heart failure - Treatment https://www.nhs.uk/conditions/heart-failure/ (accessed Apr. 19, 2024).

(4) American Heart Association Inc. Heart Attack Treatment https://www.heart.org/en/health-topics/heart-attack/treatment-of-a-heart-attack (accessed Apr. 29, 2024).

(5) Rabkin, E. et al. *Cardiovascular Pathology* **2002**, *11*, 305–317.

(6) Koninckx, R. et al. *Cardiovascular Research* **2013**, *97*, 413–23.

(7) The International Society for Stem Cell Research Types of Stem Cell Treatments https://www.aboutstemcells.org/info/what-are-stem-cell-treatments (accessed Apr. 29, 2024).

(8) Chowdhury, M. A. et al. *Frontier in Physiology* **2023**, *14*, 1344885.

(9) Hoeeg, C. et al. *Gels* **2021**, *7*, 7.

(10) Li, J. et al. *Journal of the American Heart Association* **2021**, *10*, e020402.

(11) Fanton, Y. et al. *International Journal of Cardiology* **2015**, *201*, 10–9.

(12) Ikada, Y. *Journal of the Royal Society Interface* **2006**, *3*, 589–601.

(13) Wang, H. et al. *Advanced Functional Materials* **2017**, *27*, 1605609.

(14) Singh, S. et al. *Materials Today: Proceedings* **2023**, *78*, 138–144.

(15) Lee, K. Y. et al. *Chemical Reviews* **2001**, *101*, 1869–1880.

(16) Ferreira, N. N. et al. *European Polymer Journal* **2018**, *99*, 117–133.

(17) Arani, A. et al. *Journal of Magnetic Resonance Imaging* **2017**, *46*, 1361–1367.

(18) Emig, R. et al. *Biophysical Reviews* **2021**, *13*, 587–610.

(19) Saravanakumar, K. et al. *International Journal of Biological Macromolecules* **2022**, *222*, 2744–2760.

(20) Yasin, A. et al. *Frontier of Bioengineering Biotechnology* **2022**, *10*, 910290.

(21) Yoon, S. J. et al. *Journal of Biomedical Materials Research Part B Applied Biomaterials* **2009**, *91*, 163–71.

(22) Lyu, Y. et al. *ACS Biomaterials Science & Engineering* **2020**, *6*, 6926–6937.

(23) Nettles, D. L. et al. *Advanced Drug Delivery Reviews* **2010**, *62*, 1479–85.

(24) MuñOz, E. M. et al. *Arteriosclerosis, Thrombosis, and Vascular Biology* **2004**, *24*, 1549–1557.

(25) Woods, A. et al. *Molecular Biology of the Cell* **1993**, *4*, 605–13.

(26) Xu, J. et al. *Molecules* **2019**, *24*, 3005.

(27) McDaniel, J. R. et al. *Biomacromolecules* **2010**, *11*, 944–952.

(28) Suhar, R. A. et al. *Biomacromolecules* **2023**, *24*, 5926–5939.

(29) ThermoFisher HisPur Ni-NTA Resin User Guide https://assets.thermofisher.com/TFS-Assets/LSG/manuals/MAN0011700_HisPur_NiNTA_Resin_UG.pdf (accessed Dec. 29, 2023).

(30) Sweet, C. et al. *Biomacromolecules* **2021**, *22*, 1990–1998.

(31) Mahmood, T. et al. *North American Journal of Medicine and Science* **2012**, *4*, 429–34.

(32) Shen, C.-H. In *Diagnostic Molecular Biology (Second Edition)*; Academic Press: 2023; Chapter 9 - Quantification and analysis of proteins, pp 231–257.

(33) ThermoFisher Scientific BCA Assay and Lowry Assays https://www.thermofisher.com/be/en/home/life-science/protein-biology/protein-assays-analysis/protein-assays/bca-protein-assays.html (accessed Dec. 29, 2023).

(34) Maiz-Fernández, S. et al. *Gels* **2022**, *8*, 477.

(35) Joo, H. et al. *Pharmaceutics* **2021**, *13*.

(36) Grosu, I. G. et al. *Polymers (Basel)* **2023**, *15*, 2825.

(37) Thermo Scientific TNBSA Product Instructions https://assets.thermofisher.com/TFS-Assets/BID/manuals/D00386~.pdf (accessed Jan. 15, 2024).

(38) Lavrador, P. et al. *Advanced Healthcare Materials* **2020**, *9*, 1901860.

(39) Afinjuomo, F. et al. *Polymers (Basel)* **2020**, *12*, 1025.

(40) Tong, W. et al. *Journal of Pharmaceutical and Biomedical Analysis Open* **2023**, *2*, 100022.

(41) Pandit, A. H. et al. *International Journal of Biological Macromolecules* **2019**, *137*, 853–869.

(42) Shoham, N. et al. *Journal of the Mechanical Behavior of Biomedical Materials* **2013**, *28*, 320–331.

(43) Thermo Scientific Product Information: PspFI https://www.thermofisher.com/document-connect/document-connect.html?url=https://assets.thermofisher.com/TFS-Assets%2FLSG%2Fmanuals%2FMAN0012611_FastDigest_PspFI_UG.pdf (accessed May 30, 2024).

(44) Thermo Scientific Product Information: XhoI https://www.thermofisher.com/document-connect/document-connect.html?url=https://assets.thermofisher.com/TFS-Assets%2FLSG%2Fmanuals%2FMAN0012491_FastDigest_XhoI_1200uL_UG.pdf (accessed May 27, 2024).

(45) Thermo Scientific Product Information: SalI https://www.thermofisher.com/document-connect/document-connect.html?url=https://assets.thermofisher.com/TFS-Assets%2FLSG%2Fmanuals%2FMAN0012485_FastDigest_SalI_UG.pdf (accessed May 27, 2024).

(46) Thermo Scientific Product Information: T4 DNA Ligase https://assets.thermofisher.com/TFS-assets/LSG/manuals/MAN0011990_T4_DNA_Ligase_5_Weiss_200_Weiss_U_UG.pdf (accessed May 22, 2024).

(47) Addgene Bacterial transformation https://www.addgene.org/protocols/bacterial-transformation/ (accessed May 22, 2024).

(48) Thermo Scientific Product Information: Phire Hot Start II DNA Polymerase https://assets.thermofisher.com/TFS-Assets/LSG/manuals/MAN0012385_Phire_HotStartII_DNAPolymerase_200rxns_UG.pdf (accessed May 22, 2024).

(49) Thermo Scientific User Guide: FastAP™ Thermosensitive Alkaline Phosphatase https://assets.thermofisher.com/TFS-Assets/LSG/manuals/MAN0012876_FastAP_Thermo_Alkaline_Phosphatase_ef0651_UG.pdf (accessed May 30, 2024).

(50) Haider, S. R. et al. *Methods in Molecular Biology* **2012**, *869*, 81–91.

(51) Su, C. et al. *Asian Journal of Chemistry* **2014**, *26*, 5301–5304.

(52) Macdougall, L. J. et al. *Biomacromolecules* **2018**, *19*, 1378–1388.

Supporting information

Table S1. Plasmid library with all possible tetramer combinations of RGD and HBD in ELPs starting from dimers. In bold are the combinations used in current experiments, in green are the remainder variants of which plasmids were already made. In red are the variants which still needed to be synthesized.

Variants	RR	RH	HR	HH
RR	**RRRR**	RRRH	RRHR	RRHH
RH	RHRR	RHRH	**RHHR**	**RHHH**
HR	**HRRR**	**HRRH**	HRHR	HRHH
HH	HHRR	HHRH	HHHR	**HHHH**

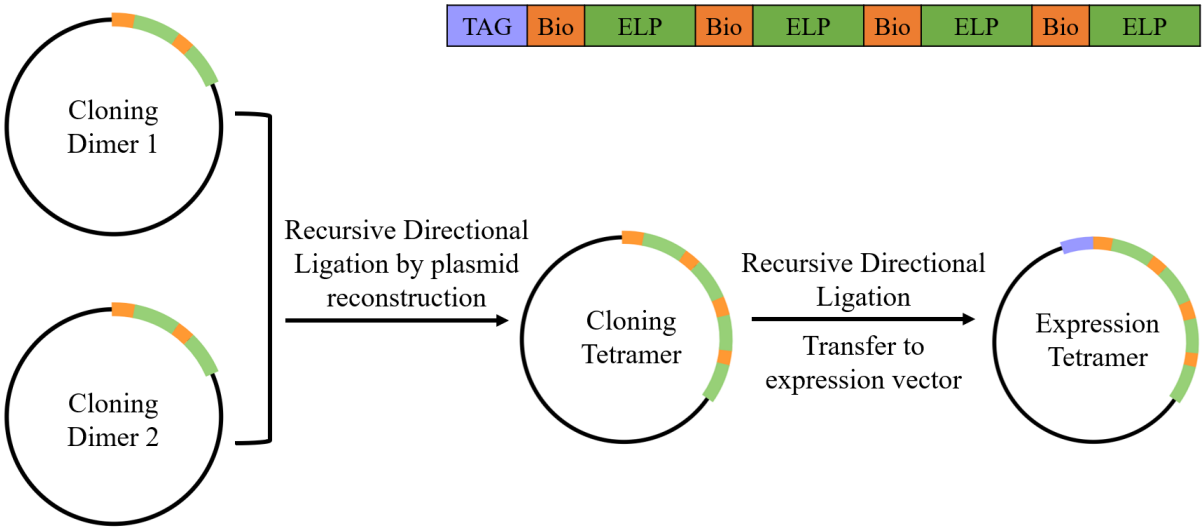

Figure S1. Conceptual figure of the tetramer insert process, starting from dimers in a cloning vector and ending with a tetramer in an expression vector. Recursive directional ligation by plasmid reconstruction is performed to obtain the tetramer in the cloning vector. Subsequently, a recursive directional ligation is performed to transfer the tetramer from a cloning to an expression vector.

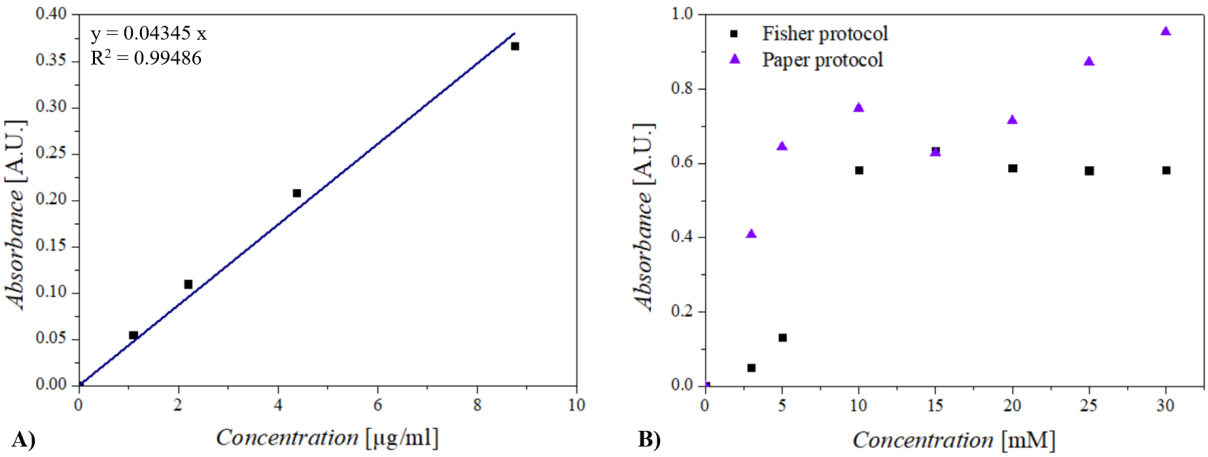

Figure S2. TNBS assay **A)** calibration curve of glycine model system, **B)** calibration results of *tert*-butyl carbazate.

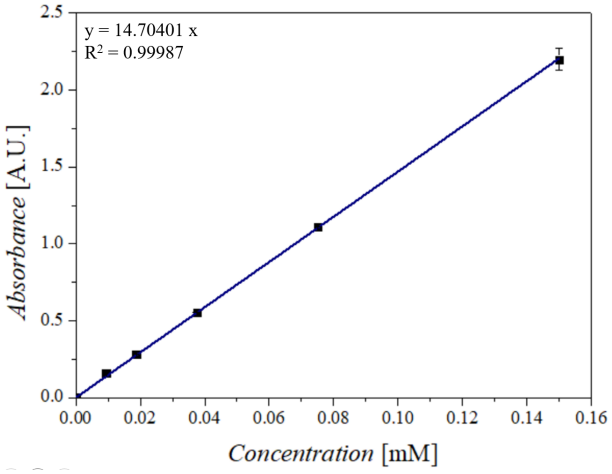

Figure S3. MBTH assay calibration curve of *para*-formaldehyde.

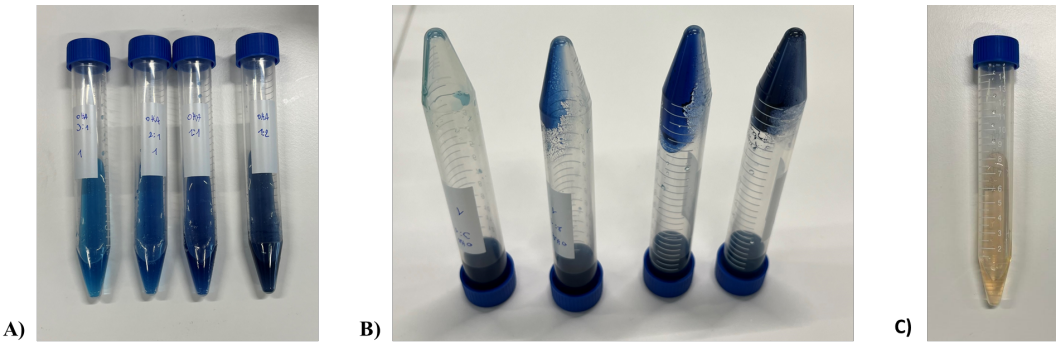

Figure S4. MBTH assay precipitation. From left to right HA:oxidant ratio of 3:1, 2:1, 1:1, and 1:2. **A)** Samples before centrifugation. An increasing blue color with increasing amount of reacted oxidant. **B)** Samples after centrifugation. With an increasing amount of oxidant, more precipitation is observed. **C)** Observed dissolution of the precipitation and color change when adding ethylenediaminetetraacetic acid, which suggests complexation of the Fe^{3+} ions with the oHA.

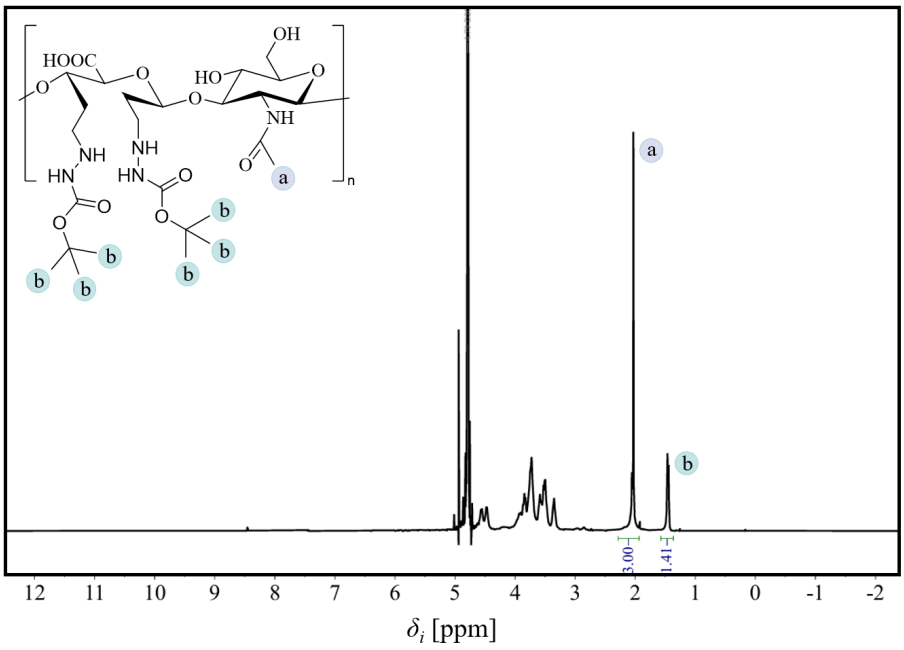

Figure S5. ^{1}H-NMR of oHA 1:1 that has reacted with *tert*-butyl carabazate, followed by the reduction of $NaCNBH_3$ for the determination of the degree of oxidation. ^{1}H-NMR in D_2O (400 MHz, 298 K), integrated values used for the calculations for the degree of oxidation are indicated.

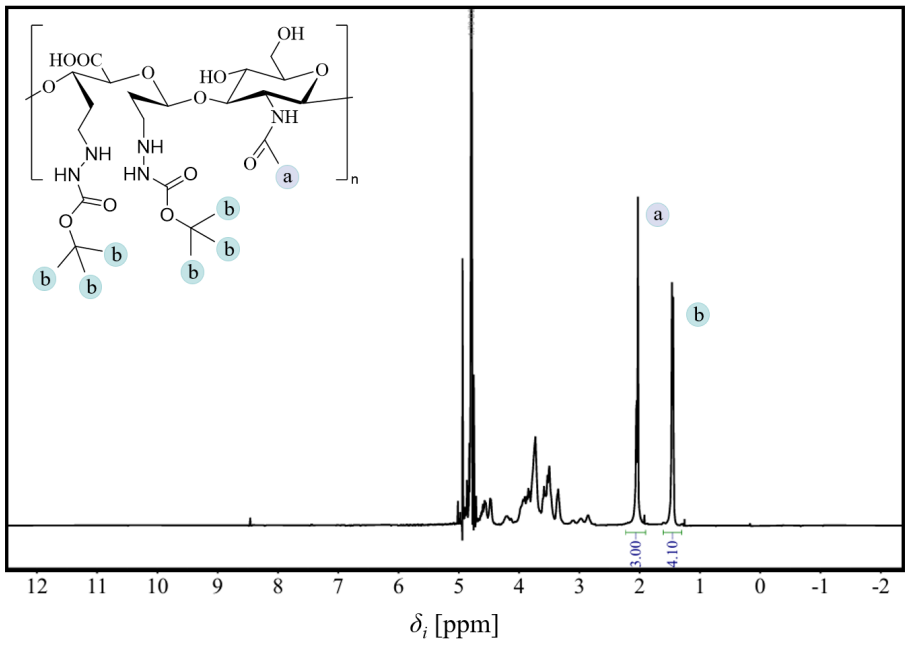

Figure S6. ^{1}H-NMR of oHA 1:2 that has reacted with *tert*-butyl carabazate, followed by the reduction of $NaCNBH_3$ for the determination of the degree of oxidation. ^{1}H-NMR in D_2O (400 MHz, 298 K), integrated values used for the calculations for the degree of oxidation are indicated.

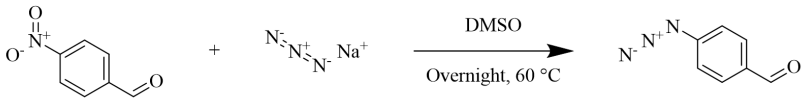

Scheme S1. Reaction scheme of the formation of 4-azidobenzaldehyde starting from 4-nitrobenzaldehyde.

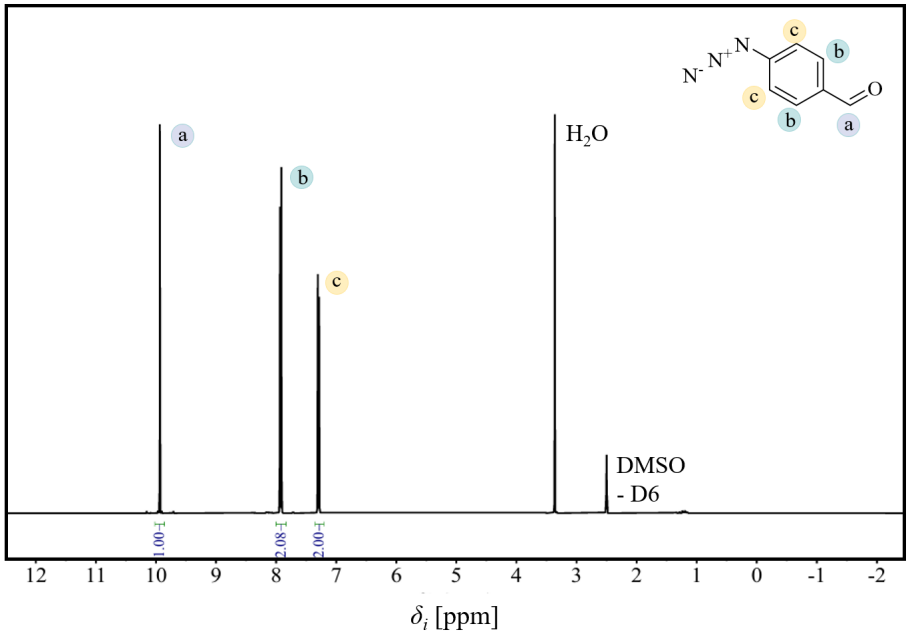

Figure S7. [1]H-NMR of 4-azidobenzaldehyde in DMSO-D6 (400 MHz, 298 K).

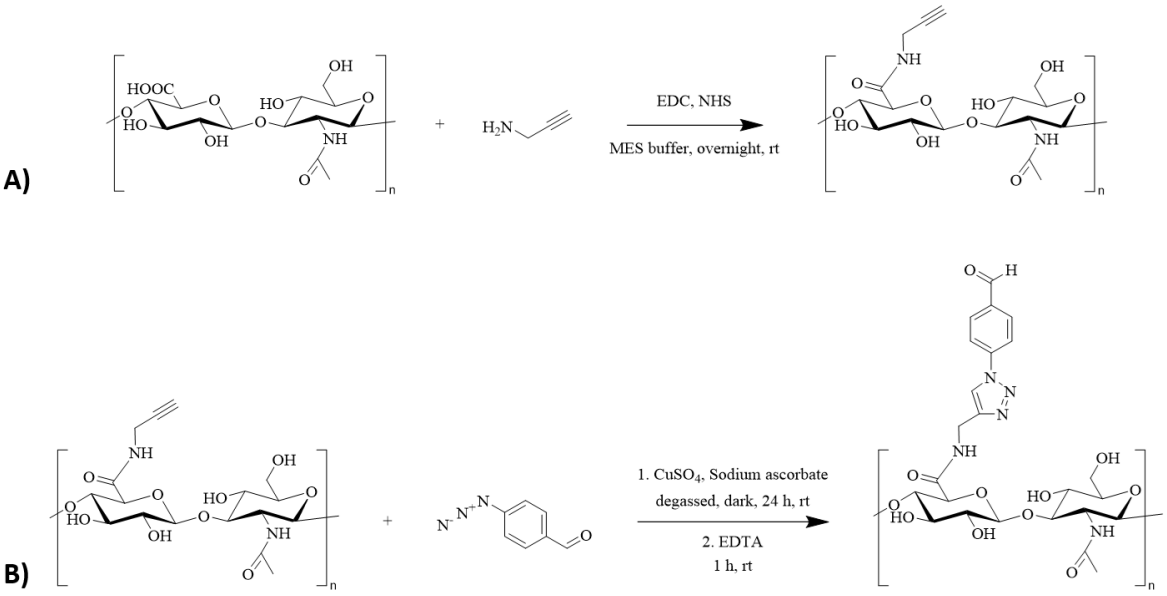

Scheme S2. Reaction scheme of reaction to introduce an aldehyde functional group in hyaluronic acid with 4-nitrobenzaldehyde. **A)** EDC-NHS coupling to functionalize the HA with an alkyne functional group. **B)** Copper click chemistry between alkyne functionalized HA and 4-azidobenzaldehyde.

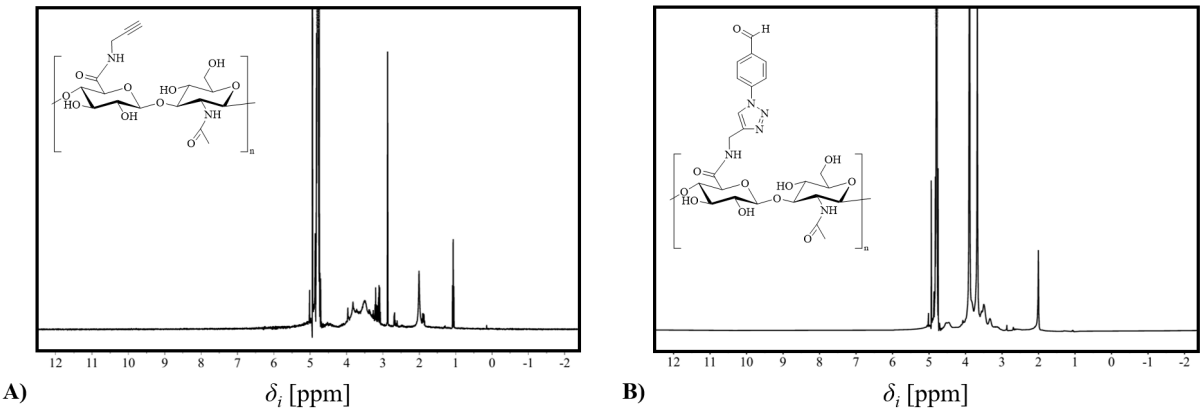

Figure S8. ^{1}H-NMR of **A)** alkyne functionalized HA and **B)** HA-benzaldehyde in D_2O (400 MHz, 298 K)

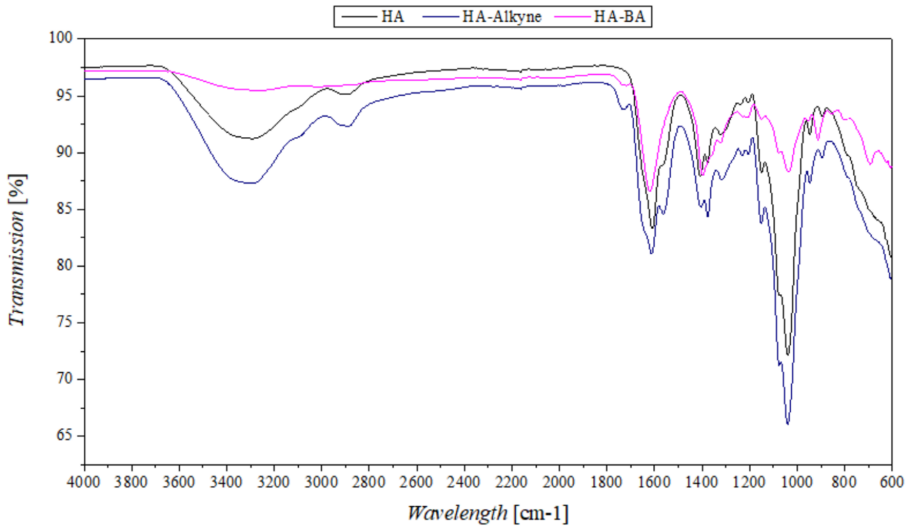

Figure S9. FTIR spectra of hyaluronic acid compared to the alkyne functionalized HA (HA-Alkyne) and the HA functionalized with benzaldehyde (HA-BA).

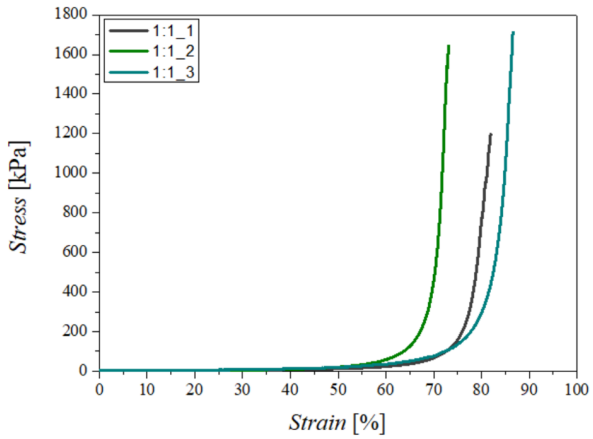

Figure S10. Stress-strain curve for the compression test of the 1:1 oHA 6 w/v % - ADH 4 w/v % hydrogels in triplicate.

Table S2. FastDigest restriction reaction mixture. For the reaction of dimers to tetramer in the pUC18 vector, PspFI was used as enzyme 1 for both dimers; for enzyme 2, XhoI was used to restrict one dimer, and SalI was used to restrict the other dimer. When going from a pUC18 vector to the pET15b vector, XhoI and SalI were the enzymes used.

	Tetramer in pUC18	Tetramer in pET15b
DNA	2 µg	3 µg
Enzyme 1	1 µL	2 µL
Enzyme 2	1 µL	2 µL
Fast digest 10x buffer	3 µL	4 µL
Total volume	30 µL	40 µL

Table S3. PCR thermal conditions.

	M13/pUC primers		T7 primers	
PCR conditions	Temperature	Time	Temperature	Time
Start	98 °C	3 min.	98 °C	2 min.
35 cycles	98 °C	5 sec.	98 °C	5 sec.
	58 °C	5 sec.	50 °C	5 sec.
	72 °C	15 sec.	72 °C	20 sec.
End	72 °C	3 min.	72 °C	3 min.

Table S4. Restriction pET15b reaction mixture.

	Volume
Vector	1 µg
XhoI	2 µL
fastAP	1 µL
Fast digest 10x buffer	4 µL
Total volume	40 µL